1 **Trivalent NDV-HXP-S vaccine protects against phylogenetically**

2 **distant SARS-CoV-2 variants of concern in mice**

3

4 Irene González-Domínguez[1‡], Jose Luis Martínez[1‡], Stefan Slamanig[1], Nicholas Lemus[1],
5 Yonghong Liu[1], Tsoi Ying Lai[1], Juan Manuel Carreño[1], Gagandeep Singh (a)[1], Gagandeep
6 Singh (b)[1,2], Michael Schotsaert[1,2], Ignacio Mena[1,2], Stephen McCroskery[1], Lynda Coughlan[3,4],
7 Florian Krammer[1,5], Adolfo García-Sastre[1,2,5,6,7], Peter Palese[1,6*] and Weina Sun[1*]
8
9 [1] Department of Microbiology, Icahn School of Medicine at Mount Sinai, New York, NY

10   10029, USA

11 [2] Global Health Emerging Pathogens Institute, Icahn School of Medicine at Mount Sinai, New

12   York, NY 10029, USA

13 [3] Department of Microbiology and Immunology, University of Maryland School of Medicine,

14   Baltimore, MD, USA.

15 [4] Center for Vaccine Development and Global Health (CVD), University of Maryland School

16   of Medicine, Baltimore, MD, USA.

17 [5] Department of Pathology, Molecular and Cell-Based Medicine, Icahn School of Medicine at

18   Mount Sinai, New York, NY 10029, USA

19 [6] Department of Medicine, Icahn School of Medicine at Mount Sinai, New York, NY 10029,

20   USA

21 [7] The Tisch Cancer Institute, Icahn School of Medicine at Mount Sinai, New York, NY 10029,

22   USA

23

24 [‡] Equally contributed

25 *Correspondence: peter.palese@mssm.edu and weina.sun@mssm.edu

26

27

Abstract

Equitable access to vaccines is necessary to limit the global impact of the coronavirus disease 2019 (COVID-19) pandemic and the emergence of new severe acute respiratory syndrome coronavirus 2 (SARS-CoV-2) variants. In previous studies, we described the development of a low-cost vaccine based on a Newcastle Disease virus (NDV) expressing the prefusion stabilized spike protein from SARS-CoV-2, named NDV-HXP-S. Here, we present the development of next-generation NDV-HXP-S variant vaccines, which express the stabilized spike protein of the Beta, Gamma and Delta variants of concerns (VOC). Combinations of variant vaccines in bivalent, trivalent and tetravalent formulations were tested for immunogenicity and protection in mice. We show that the trivalent preparation, composed of the ancestral Wuhan, Beta and Delta vaccines, substantially increases the levels of protection and of cross-neutralizing antibodies against mismatched, phylogenetically distant variants, including the currently circulating Omicron variant.

46

Introduction

48 Severe acute respiratory syndrome coronavirus 2 (SARS-CoV-2) is the causative agent of the
49 current coronavirus disease 2019 (COVID-19). Since the beginning of the pandemic, the
50 emergence of new variants of concern (VOC) has threatened the protection conferred by
51 vaccines based on the original strain (Figure 1) [1]. In December 2020, the Alpha variant
52 (B.1.1.7) and Beta variant (B.1.351) were declared VOC and spread over the world, followed by
53 the Gamma strain (P.1) that was declared a VOC in January 2021. Both Beta and Gamma
54 variants exhibited notable resistance to neutralizing antibodies raised against the original strain
55 in humans [1, 2]. In May 2021, a strong pandemic wave in India gave rise to a new VOC: the
56 Delta variant (B.1.617.2). This new VOC harbored different mutations in the spike that
57 significantly reduced its sensitivity to neutralizing antibodies, and increased transmissibility
58 quickly replacing the previous variants worldwide (Figure 1B) [1, 3]. In November 2021, a new
59 VOC named Omicron appeared in South Africa. Since then, Omicron has taken over worldwide,
60 replacing the Delta variant [4]. Compared to the previous VOC, Omicron presents the highest
61 number of mutations in the spike protein and has shown the highest drop-in neutralization
62 activity [5, 6]. Currently, the Omicron sub-lineage BA.2, seems to show even more immune
63 evasion and transmissibility [7-9].

64 Despite the unprecedented, rapid development of COVID-19 vaccines, only ~63% of the global
65 population are fully vaccinated (as of 14th March 2022) [6]. Hence, there is still a need for
66 COVID-19 vaccines that can be produced locally in low- and middle-income countries (LMICs),
67 where the vaccination rates are the lowest worldwide [6]. In previous work, we developed a
68 vaccine candidate named NDV-HXP-S [10] that can be manufactured like influenza virus
69 vaccines at low cost in embryonated chicken eggs in facilities located globally [11]. This
70 vaccine is based on an avirulent Newcastle disease virus (NDV) strain which presents a SARS-
71 CoV-2 spike protein stabilized in its prefusion-conformation by the introduction of six proline
72 mutations (HexaPro, HXP-S) [4, 12] and elimination of the furin cleavage site. NDV-HXP-S
73 can be used as live vaccine [11, 13, 14] or as an inactivated vaccine [11, 15]. Clinical trials with
74 a live version are ongoing in Mexico (NCT04871737) and the US (NCT05181709), while the
75 inactivated vaccine is being tested in Vietnam (NCT04830800), Thailand (NCT04764422) and
76 Brazil (NCT04993209). Interim results from the initial Phase I/II trials have demonstrated that
77 the vaccine was safe and immunogenic [15-17].

78 Here, we present the development of NDV-HXP-S variant vaccines displaying the VOC spike
79 proteins of Beta, Gamma and Delta. We tested the immunogenicity and protection induced by
80 vaccination with inactivated NDV-HXP-S variants in mice. We observed that variant-specific
81 vaccines induced the strongest antibody responses towards the homologous SARS-CoV-2 VOC.
82 Furthermore, we found that a combination of multivalent NDV-HXP-S with the Wuhan, Beta

83 and Delta provided a broader protection against a panel of VOC than the monovalent

84 formulations.

85

86 **Results**

87 **Design and production of NDV-HXP-S variant vaccines**

88 NDV-HXP-S variant vaccines based on three VOC, Beta (B.1.351), Gamma (P.1) and Delta

89 (B.1.617.2), were rescued using reverse genetics in mammalian cell cultures and further

90 amplified in specific-pathogen free (SPF) embryonated chicken eggs as previously described

91 (Figure 2) [11]. The nucleotide sequence of the constructs was codon-optimized for mammalian

92 host expression. The HXP-S sequence was inserted between the P and M genes of the NDV

93 genome. We removed the polybasic cleavage site (^{682}RRAR^{685}) and replaced the transmembrane

94 domain (TM) and cytoplasmic tail (CT) of the spike with those from the fusion (F) protein of La

95 Sota NDV. The HXP mutations were introduced into the spike S2 region of all three variant S

96 proteins to improve their stability as reported previously (Figure 2A & 2B) [12]. In addition, we

97 found that a completely cleaved Delta spike was observed when the Delta specific S-P681R

98 mutation was included. Therefore, we kept the 681 as proline to ensure the homogeneity of

99 prefusion conformation (S0) (Figure 2C).

100 Research-grade beta-propiolactone (BPL) inactivated NDV-HXP-S variant vaccine preparations

101 were produced. Virus was concentrated from the harvested allantoic fluid through a sucrose

102 cushion and resolved on a sodium dodecyl–sulfate polyacrylamide gel (SDS–PAGE) with

103 Coomassie Blue staining to evaluate the presence of all NDV-HXP-S proteins. NDV-HXP-S

104 variants showed an extra band between 160 kDa and 260 kDa below the L protein of the NDV

105 that corresponds to the size of the uncleaved spike (S0, Figure 2D) [11].

106

107 **NDV-HXP-S variant vaccines protect against homologous challenge in mouse models**

108 The immunogenicity and *in vivo* protection of the new NDV-HXP-S Beta and Gamma vaccine

109 candidates was first evaluated in BALB/c mice transduced with a non-replicating human

110 adenovirus 5 expressing human angiotensin-converting enzyme 2 (Ad5-hACE2) (Figure 3A). A

111 two-dose intramuscular (IM) vaccination regimen with a total protein content of 1 μg per mouse

112 of purified NDV-HXP-S vaccine candidate with a 3-week period between doses was followed.

113 Three weeks after the boost, BALB/c mice were transduced by intranasal (IN) administration of

114 the Ad5-hACE2 and five days later mice were challenged with SARS-CoV-2 viruses via the IN

115 route, as previously described [18]. Two days after challenge, viral titers in the lung

116 homogenates were quantified by plaque assays. Vaccination with wild type NDV was used as

117 negative control (Figure 3B).

118 A viral titer reduction of 2,237-fold, 2,015-fold and 285-fold was obtained in the homologous

119 challenge using monovalent vaccination regimens with Wuhan, Beta and Gamma NDV-HXP-S

120   vaccines compared to the negative control, respectively (*p.value <0.05 versus the neg.control*,

121   Figure 3C). Heterologous protection with Wuhan NDV-HXP-S against Beta and Gamma

122   challenge was observed with a viral titer reduction of 51-fold and 120-fold compared to the

123   negative control, respectively, in agreement with previous studies [11]. Beta NDV-HXP-S

124   vaccine showed cross-protection against the Gamma variant challenge, and *vice versa*. However,

125   an asymmetric weaker protection of Beta and Gamma vaccines was observed against the Wuhan

126   challenge.

127   Together with the *in vivo* challenge study, mice were bled 3-weeks after boost to measure the

128   spike-specific IgG levels. Antibody titers after vaccination against Wuhan, Beta and Gamma

129   spikes were compared in Figures 3D-F, respectively. Wuhan spike-specific IgG serum antibody

130   titers were higher after the vaccination with the original construct compared to Beta and Gamma

131   NDV-HXP-S vaccinations (Figure 3D). Similar Beta and Gamma spike-specific antibody titers

132   were obtained with all three vaccination regimens (Figure 3E-F). These results correlate with

133   the challenge against the three viruses, where a similar cross-protection was obtained against

134   Beta and Gamma challenges with all three vaccination regimens. As the Delta variant emerged,

135   we also measured post-boost serum antibodies against the Delta spike (Figure 3G). Compared to

136   the other spike-specific titers, the levels of cross-reactive antibodies against the Delta spike were

137   reduced in all three vaccination groups, suggesting a higher drop in protection against this

138   variant with the current constructs tested.

139

Trivalent and tetravalent NDV-HXP-S variant vaccinations increase protection *in vivo*

against phylogenetically distant SARS-CoV-2 variants

142   Following the characterizations of Beta and Gamma NDV-HXP-S vaccines, the Delta VOC

143   appeared in India and rapidly replaced the other variants (Figure 1B). When the Delta vaccine

144   construct was generated, a second mouse immunization and challenge study was performed

145   testing vaccine formulations containing the Delta component (Figure 4A). Based on the

146   previous results, the following groups were evaluated: monovalent Wuhan, monovalent Delta,

147   bivalent Wuhan and Delta, sequential vaccination with a first dose of Wuhan followed by Delta,

148   trivalent (Wuhan, Delta and Beta) and tetravalent (Wuhan, Delta, Beta and Gamma). In all cases,

149   the vaccination dose was 1 µg of total protein (Figure 4B).

150   In this study, we wanted to test not only the protection against homologous challenge, but also

151   against a phylogenetically distant SARS-CoV-2 variant, which is unmatched to any vaccine

152   component. To do so, animals in each group were divided into 3 subgroups and challenged with

153   Wuhan, Delta and Mu variants (Figure 4C). As expected, Wuhan and Delta showed protection

154   against its homologous virus challenge. Of note, bivalent, trivalent and tetravalent vaccines

155   showed comparable levels of protection as the homologous monovalent vaccines against

156   Washington 1 (Wuhan-like) and Delta challenges. Viral titers were reduced in trivalent

157 condition 21,845-fold and 3,119-fold compared to the negative control in Wuhan and Delta

158 challenges, respectively. However, sequential vaccination regimen was shown to be less

159 protective, with only a 54-fold mean titer reduction in Delta challenge. In the case of the Mu

160 challenge, trivalent formulation was proven to be the best with a titer reduction of 594-fold

161 (Figure 4C, *p.value <0.0001 compared to the neg. control)*. This reduction was 2.4 times higher

162 than any of the other vaccination strategies tested including that of the tetravalent preparation

163 (for discussion see below).

164 Considering the new emergence of the Omicron variant, we decided to compare the neutralizing

165 activity of post-boost serum antibodies against the Wuhan, Delta, Beta and Omicron variants in

166 authentic virus neutralization assays (Figure 4D). A similar 50% inhibitory dilution (ID_{50}) was

167 obtained against Wuhan in all vaccinated groups except for Delta (0.4-fold compared to Wuhan).

168 In the case of Delta microneutralization, the neutralizing activity was increased in the trivalent

169 and tetravalent (2.0-fold and 2.5-fold compared to the ancestral strain, respectively), whereas

170 Wuhan alone and sequential showed a smaller neutralizing activity . A similar ID_{50} was

171 obtained against Beta with monovalent, bivalent, and sequential strategies, whereas it was

172 increased 2.5-fold and 2.7-fold in the trivalent and tetravalent groups, respectively. Little

173 neutralizing activity was found against Omicron in the Wuhan vaccination, whereas the Delta

174 vaccine showed a 5.6-fold increase compared to the vaccination with the monovalent Wuhan

175 NDV-HXP-S. The neutralization titer against the Omicron was further increased by the trivalent

176 and tetravalent vaccines (9.3-fold and 11.0-fold compared to the monovalent ancestral NDV-

177 HXP-S vaccine group, respectively).

178

179 **Trivalent and tetravalent NDV-HXP-S vaccinations increase antibody binding to the spike**

180 **of SARS-CoV-2 variants**

181 In the attempt to elucidate the mechanism of cross-protection induced by the multivalent

182 vaccine formulations, antibody-binding profiles were measured against a panel of SARS-CoV-2

183 spike proteins, including the Wuhan, Delta, Alpha, Beta, Gamma and Omicron (Figure 5A-B).

184 Wuhan and Delta spike-specific IgG levels were comparable among all vaccination groups. In

185 the case of Beta, an increase of 2.9-fold and 1.9-fold were observed in the trivalent and

186 tetravalent vaccination compared to monovalent Wuhan group, respectively. An increase was

187 also observed against Alpha (1.7-fold) and Gamma spikes (1.5-fold) in the trivalent condition

188 (Figure 5A). Finally, vaccinated mice sera were also tested against Omicron spike. Omicron

189 presents almost 40 different amino acid changes and deletions. A general reduction in antibody

190 titers against Omicron spike was found in all groups compared to the other spikes tested (Figure

191 5A, see Y axes). Despite this drop, the addition of Delta and Beta increased spike-specific IgG

192 titers against Omicron: 2.4-fold in the Delta vaccinated group, 5.7-fold with trivalent and 3.0

193 times with the tetravalent vaccinated group compared to the Wuhan vaccinated group, which

194 correlates with the neutralization titers against Omicron (Figure 4D). Overall, the trivalent

195 immunization regimen induced the highest titers of spike-specific antibody levels across all the

196 variants tested (Figure 5B).

197

198 **Discussion**

199 The COVID-19 pandemic has seen an unprecedented race in the development of next

200 generation vaccines. Compared to the traditionally slow vaccine development, novel vaccine

201 platforms such as Moderna and Pfizer/BioNTech's mRNA vaccines or Janssen and

202 AstraZeneca's adenovirus-based vaccines have been authorized for emergency use in one year

203 [6, 19]. Despite this tremendous effort, only ~63% of the global population has been fully

204 vaccinated, largely due to unequal vaccine distribution (as of 14th of March 2022) [6]. This fact,

205 together with the continuing emergence of VOC, which present a higher transmissibility and

206 resistance to vaccine-mediated protection, has caused thousands of deaths per day since the

207 beginning of the pandemic. In the last few months, the situation has worsened with the arrival of

208 Omicron, where the world has experienced the highest number of daily cases to date [6].

209 With the NDV-based vaccine platform, we successfully constructed variant-specific vaccines

210 for Beta, Gamma, and Delta variants. In mice, variant-specific vaccines effectively conferred

211 protection against homologous viruses. To test if the co-administration of prior variants could

212 potentially induce cross-protective immune responses against unmatched and antigenically

213 distinct lineages, we examined bivalent, sequential, trivalent, and tetravalent formulations of

214 inactivated NDV-HXP-S variant vaccines. Bivalent vaccination with Wuhan and Delta showed

215 an improved immunogenicity compared to the monovalent vaccinations, whereas the sequential

216 strategy, where the same Wuhan and Delta candidates were given in consecutive doses, showed

217 no improvement compared to the monovalent Wuhan NDV-HXP-S group. Comparable levels

218 of protection by a sequential administration of variant-like vaccines versus a booster dose of the

219 original vaccine candidate have been observed in other preclinical studies [20, 21], however the

220 long-term benefits of these heterologous boosters are still to be investigated.

221 Trivalent and tetravalent formulations presented synergistic responses in terms of the protection

222 to the unmatched Mu VOC in challenge studies in mice (Figure 4C). Similarly, *in vitro*

223 microneutralization assays have always demonstrated an increase in cross-neutralizing

224 antibodies against all viruses tested, including against the Omicron variant (Figure 4D).

225 Phylogenetically, Wuhan, Beta, Gamma and Delta are distinct from each other. A multivalent

226 vaccination may induce several repertoires of cross-neutralizing antibodies that might target

227 some common epitopes with other unmatched variants. There are several explanations to this

228 phenomenon. One possibility is that each variant contributes with unique neutralizing epitope(s)

229 that expand the repertoire of neutralization responses. It is also possible that conserved

230 neutralizing epitopes shared by all the variants are more immunodominant in one variant than

231 the other due to conformational halosteric changes resulting from spike mutations. Therefore,
232 one variant may have induced more cross-neutralizing antibodies than the other. When trivalent
233 and tetravalent vaccination regimens are compared between with each other, no advantage of
234 the tetravalent regimen compared to trivalent was observed in the *in vivo* challenge experiment
235 in mice. The dose reduction from 0.33 μg to 0.25 μg per variant or the lower immunogenicity of
236 the Gamma vaccine might explain these results.

237 The NDV-HXP-S vaccine has proven its safety and immunogenicity in several preclinical and
238 clinical studies. As an egg-based vaccine, NDV-HXP-S could be produced using the egg-based
239 influenza virus vaccine manufacturing capacities located worldwide. Sparrow and colleagues
240 estimated that influenza virus vaccine manufacturing capacities on its own can produce billions
241 of doses annually [10]. Here, vaccination with a trivalent formulation in mice was performed by
242 maintaining the total dose as that of the monovalent vaccine (1μg of total protein). Hence, the
243 manufacturing capabilities required to produce this new formulation will remain the same.

244 In summary, we present the development of novel NDV-HXP-S variant vaccines and test their
245 combination in a trivalent formulation to extend the generation of neutralizing antibodies
246 against unmatched VOCs. This formulation exceeds the breadth of protection of the other
247 formulations we have tested so far. This is of special interest because Omicron (B.1.1.529 or
248 BA.1) has quickly diverged into different sub-lineages (BA.1.1, BA.2 and BA.3) and has gained
249 prevalence globally (www.nextstrain.org/ncov). A variant-specific vaccine of any platform
250 comes with an intrinsic disadvantage. It can only be used after the new vaccine candidate is
251 produced and authorized by the health authorities. We believe that a more thorough selection
252 and testing of several variant vaccines in multivalent formulations might be an effective strategy
253 for vaccination against future SARS-CoV-2 variants.
254

255 **Data availability**
256 Data is available upon request.
257

258 **Ethics Statement**
259 All animal procedures in this study were performed in accordance with the animal protocol that
260 was reviewed and approved by the Icahn School of Medicine at Mount Sinai Institutional
261 Animal Care and Use Committee (IACUC).
262

263 **Authors Contribution**
264 Conceptualization and design: IGD, WS, PP; NDV rescue and characterization: JLMG, SS, NL;
265 vaccine preparation and animal experiments; IGD, YL, WS; serology: IGD, TYL, SM; protein
266 and virus reagents; GS(a), GS(b), MS, IM, LC, AG-S; microneutralization assay: JMC, FK; data

267 analysis: IGD, WS, PP; first draft: IGD, WS, PP; manuscript was reviewed and approved by all
268 authors.
269

Competing interests

281 The Icahn School of Medicine at Mount Sinai has filed patent applications entitled
282 "RECOMBINANT NEWCASTLE DISEASE VIRUS EXPRESSING SARS-COV-2 SPIKE
283 PROTEIN AND USES THEREOF" which names P.P., F.K., AG-S., and W.S. as inventors. The
284 AG-S laboratory has received research support from Pfizer, Senhwa Biosciences, Kenall
285 Manufacturing, Avimex, Johnson & Johnson, Dynavax, 7Hills Pharma, Pharmamar,
286 ImmunityBio, Accurius, Hexamer, N-fold LLC, Model Medicines, Atea Pharma, Merck and
287 Nanocomposix, and AG-S has consulting agreements for the following companies involving
288 cash and/or stock: Vivaldi Biosciences, Contrafect, 7Hills Pharma, Avimex, Vaxalto, Pagoda,
289 Accurius, Esperovax, Farmak, Applied Biological Laboratories, Pharmamar, Paratus, CureLab
290 Oncology, CureLab Veterinary, Synairgen and Pfizer. The Icahn School of Medicine at Mount
291 Sinai has filed patent applications relating to SARS-CoV-2 serological assays (U.S. Provisional
292 Application Numbers: 62/994,252, 63/018,457, 63/020,503 and 63/024,436) which list Florian
293 Krammer as co-inventor. Mount Sinai has spun out a company, Kantaro, to market serological
294 tests for SARS-CoV-2. Florian Krammer has consulted for Merck and Pfizer (before 2020), and
295 is currently consulting for Pfizer, Third Rock Ventures, Seqirus and Avimex. The Krammer
296 laboratory is also collaborating with Pfizer on animal models of SARS-CoV-2. All other authors
297 declared no competing interests.
298

Materials and methods
Cells

301 DF-1, (ATCC® CRL-12203), BSRT7 [22], and VERO-E6 (ATCC, CRL-1586) were
302 maintained in Dulbecco's Modified Eagle's Medium (DMEM; Gibco, MA, USA) containing 10%

303 (vol/vol) fetal bovine serum (FBS), 100 unit/mL of penicillin, 100 µg/mL of streptomycin (P/S;

304 Gibco) and 10 mM 4-(2-hydroxyethyl)-1-piperazineethanesulfonic acid (HEPES) at 37°C with

305 5% CO_2. VERO-TMPRSS2 cells (BPS Biosciences, #78081) were maintained in DMEM

306 (Gibco) containing 10% (vol/vol) FBS, 100 unit/mL of penicillin, 100 µg/mL of streptomycin

307 (P/S; Gibco), 5 mL of Nonessential Amino Acid Solution (NEAA, Corning™ MEM, NY, USA),

308 3 µg/mL puromycin (Invivogen, CA, USA) and 0.1 mg/mL Normocin (Invivogen) at 37°C with

309 5% CO_2.

310

Plasmids

312 Spike variant mutations were introduced into the HXP-S sequence in silico and the new

313 constructs were obtained as synthetic double-stranded DNA fragments from Integrated DNA

314 Technologies, using the gBlocks® Gene Fragments service and PCR [11]. Briefly, the variant

315 HXP-S were inserted into the pNDV_LS/L289A rescue plasmid (between P and M genes) by

316 in-Fusion cloning (Clontech, CA, USA). The recombinant product was transformed into MAX

317 Efficiency™ Stbl2™ Competent Cells (Thermo Fisher Scientific, MA, USA) to generate the

318 pNDV-HXP-S rescue plasmid. The plasmid was purified using PureLink™ HiPure Plasmid

319 Maxiprep Kit (Thermo Fisher Scientific).

320

Rescue of the NDV-HXP-S

322 As described in our previous studies [23], BSRT7 cells stably expressing the T7

323 polymerase were seeded onto 6-well plates at 3 x 10^5 cell per well in duplicate. The next day,

324 cells were transfected with 2 µg of pNDV-HXP-S, 1 µg of pTM1-NP, 0.5 µg of pTM1-P, 0.5 µg

325 of pTM1-L and 1 µg of pCI-T7opt and were re-suspended in 250 µl of a modified Eagle's

326 Minimum Essential Medium (Opti-MEM; Gibco). The plasmid cocktail was then gently

327 mixed with 15 µL of TransIT LT1 transfection reagent (Mirus, GA, USA). The growth media

328 was replaced with Opti-MEM during transfection. To increase rescue efficiency, BSRT7-DF-1

329 co-culture was established the next day as described previously [24]. Specifically, transfected

330 BSRT7 and DF-1 cells were washed with warm PBS and trypsinized. Trypsinized cells were

331 neutralized with excessive amount of growth media. BSRT7 cells were mixed with DF-1 cells

332 (~1: 2.5) in a 10-cm dish. The co-culture was incubated at 37°C overnight. The next day, the

333 media was removed, and cells were gently washed with warm PBS, Opti-MEM supplemented

334 with 1% P/S and 0.1 µg/ml of (tosyl phenylalanyl chloromethyl ketone) TPCK- treated trypsin

335 was added. The co-cultures were incubated for 2 or 3 days before inoculation into 8- or 9-day-

336 old specific pathogen free (SPF) embryonated chicken eggs (Charles River Laboratories, CT,

337 USA). To inoculate eggs, cells and supernatants were harvested and homogenized by several

338 syringe strokes. One or two hundred microliters of the mixture were injected into each egg.

339 Eggs were incubated at 37 °C for 3-5 days and cooled at 4°C overnight. Allantoic fluids (AF)

340 were harvested from cooled eggs and the rescue of the viruses was determined by
341 hemagglutination (HA) assays. RNA of the rescued virus was extracted, and RT-PCR was
342 performed to amplify the cDNA segments of the viral genome. The cDNA segments were then
343 sequenced by Sanger sequencing (Psomagen, MA, USA). The genetic stability of the
344 recombinant viruses was evaluated across multiples passages in 10 days old-SPF embryonated
345 chicken eggs.

346

347 **Virus titration by EID$_{50}$ assays**

348 Fifty percent of (embryonated) egg infectious dose (EID$_{50}$) assay was performed in 9 to
349 11-day old chicken embryonated eggs. Virus in allantoic fluid was 10-fold serially diluted in
350 PBS, resulting in 10^{-5} to 10^{-10} dilutions of the virus. One hundred microliters of each dilution
351 were injected into each egg for a total of 5-10 egg per dilution. The eggs were incubated at
352 37 °C for 3 days and then cooled at 4°C overnight, allantoic fluids were collected and analyzed
353 by HA assay. The EID$_{50}$ titer of the NDV, determined by the number of HA-positive and HA-
354 negative eggs in each dilution, was calculated using the Reed and Muench method.

355

356 **Preparation of inactivated concentrated virus**

357 The viruses in the allantoic fluid were first inactivated using 0.05% beta-propiolactone
358 (BPL) as described previously [23]. To concentrate the viruses, allantoic fluids were clarified by
359 centrifugation at 4,000 rpm at 4°C for 30 min using a Sorvall Legend RT Plus Refrigerated
360 Benchtop Centrifuge (Thermo Fisher Scientific). Clarified allantoic fluids were laid on top of a
361 20% sucrose cushion in PBS (Gibco). Ultracentrifugation in a Beckman L7-65 ultracentrifuge at
362 25,000 rpm for 2 hours at 4°C using a Beckman SW28 rotor (Beckman Coulter, CA, USA) was
363 performed to pellet the viruses through the sucrose cushion while soluble egg proteins were
364 removed. The virus pellets were re-suspended in PBS (pH 7.4). The total protein content was
365 determined using the bicinchoninic acid (BCA) assay (Thermo Fisher Scientific).

366

367 **SDS-PAGE and Western Blot**

368 The concentrated NDV-HXP-S or WT NDV was mixed with Novex™ Tris-Glycine
369 SDS Sample Buffer (2X) (Thermo Fisher Scientific), NuPAGE™ Sample Reducing Agent (10 x)
370 (Thermo Fisher Scientific) and PBS at appropriate amounts to reach a total protein content. The
371 mixture was heated at 90 °C for 5 min. The samples were mixed by pipetting and loaded to a 4-
372 20% 10-well Mini-PROTEAN TGXTM precast gel. Ten microliters of the Novex™ Sharp Pre-
373 stained Protein standard (Thermo Fisher Scientific) was used as the ladder. The electrophoresis
374 was run in Tris/Glycine SDS/Buffer (Bio-Rad).
375 For comassie blue staining, the gel was washed with distilled water at room temperature several
376 times until the dye front in the gel was no longer visible. The gel was stained with 20 mL of

377   SimplyBlue^{TM} SafeStain (Thermo Fisher Scientific) for a minimum of 1 h to overnight. The

378   SimplyBlue^{TM} SafeStain was decanted and the gel was washed with distilled water several times

379   until the background was clear. Gels were imaged using the Bio-Rad Universal Hood

380   IiIMolecular imager (Bio-Rad) and processed by Image Lab Software (Bio-Rad).

381   For Western Blot, proteins were transferred onto polyvinylidene difluoride (PVDF) membrane

382   (GE Healthcare, IL, USA). The membrane was blocked with 5% dry milk in PBS containing 0.1%

383   v/v Tween 20 (PBST) for 1h at RT. The membrane was washed with PBST on a shaker 3 times

384   (10 min at RT each time) and incubated with primary antibodies diluted in PBST containing 1%

385   bovine serum albumin (BSA) overnight at 4°C. To detect the spike protein of SARS-CoV-2, a

386   mouse monoclonal antibody 2B3E5 recognizing the S1 kindly provided by Dr. Thomas Moran

387   at ISMMS was used. The HN protein was detected by a mouse monoclonal antibody 8H2

388   (MCA2822, Bio-Rad). The membranes were then washed with PBST on a shaker 3 times (10

389   min at RT each time) and incubated with sheep anti-mouse IgG linked with horseradish

390   peroxidase (HRP) diluted (1:2,000) in PBST containing 5% dry milk for 1h at RT. The

391   secondary antibody was discarded and the membranes were washed with PBST on a shaker 3

392   times (10 min at RT each time). Pierce™ ECL Western Blotting Substrate (Thermo Fisher

393   Scientific) was added to the membrane, the blots were imaged using the Bio-Rad Universal

394   Hood II Molecular imager (Bio-Rad) and processed by Image Lab Software (Bio-Rad).

395

396   **Animal experiments**

397   All the animal experiments were performed in accordance with protocols approved by

398   the Icahn School of Medicine at Mount Sinai (ISMMS) Institutional Animal Care and Use

399   Committee (IACUC). All experiments with live SARS-CoV-2 were performed in the Centers

400   for Disease Control and Prevention (CDC)/US Department of Agriculture (USDA)-approved

401   biosafety level 3 (BSL-3) biocontainment facility of the Global Health and Emerging Pathogens

402   Institute at the Icahn School of Medicine at Mount Sinai, in accordance with institutional

403   biosafety requirements.

404

405   **Mouse immunization and challenge studies**

406   Female BALB/c mice were used in all studies. Intramuscular vaccination using 1 μg of

407   total protein of inactivated NDV-HXP-S vaccine or negative control WT NDV was prepared in

408   100 μl total volume. Two immunizations were performed for all the mice with a 21-day interval.

409   For SARS-CoV-2 infection, mice were intranasally infected with 2.5×10^8 plaque forming units

410   (PFU) of Ad5-hACE2 5 days prior to being challenged with 1×10^5 PFU USA-WA1/2020

411   strain (Wuhan-like), 3.4×10^4 PFU of the hCoV-19/USA/MD-HP01542/2021 JHU strain (Beta,

412   kindly provided by Dr. Andrew Pekosz from Johns Hopkins Bloomberg School of Public

413   Health), 6.3×10^4 PFU of the hCoV-19/Japan/TY7-503/2021 strain (Gamma), 1.6×10^5 PFU of

414   the hCoV-19/USA/NYMSHSPSP-PV29995/20212021 strain (Delta, obtained from Dr. Viviana

415   Simon (Mount Sinai Pathogen Surveillance program) and 5.0×10^3 PFU of the hCoV-

416   19/USA/WI-UW-4340/2021strain2021strain (Mu, kindly provided by Dr. Michael S. Diamond

417   from Washington University Medical School in St. Louis). Viral titers in the lung homogenates

418   of mice 2 days post-infection were used as the readout for protection. Briefly, the lung lobes

419   were harvested from a subset of animals per group and homogenized in 1 mL of sterile PBS.

420   Viral titers in the lung homogenates were measured by plaque assay on Vero-E6 or Vero-

421   TMPRSS2 cells. Blood was collected by submandibular vein bleeding. Sera were isolated by

422   low-speed centrifugation and stored at -80°C before use.

423

424   **Recombinant proteins**

425   Recombinant WA1, Beta, Alpha and Omicron spike proteins and recombinant WA1,

426   Beta, Alpha, Gamma, Delta and Omicron RBDs were generated and expressed in Expi293F

427   cells (Life Technologies, Thermo Fisher Scientific) as previously described [25, 26]. Proteins

428   were then purified after transient transfections with each respective plasmid. Briefly, the

429   mammalian-cell codon-optimized nucleotide sequence of a soluble spike protein (amino acids

430   1-1,213) lacking the polybasic cleavage site, carrying two stabilizing mutations (K986P and

431   V987P), a signal peptide, and at the C-terminus a thrombin cleavage site, a T4 fold-on

432   trimerization domain, and a hexahistidine tag was cloned into the mammalian expression vector

433   pCAGGS. https://www.beiresources.org/).Protein was purified using gravity flow purification

434   with Ni-nitrilotriacetic acid (NTA) agarose (Qiagen, Germany) and concentrated and buffer

435   exchanged in Amicon centrifugal units (EMD Millipore, MA, USA). The purified recombinant

436   proteins were analyzed via reducing sodium dodecyl sulfate-polyacrylamide gel electrophoresis

437   (SDS-PAGE). The desired protein folding was confirmed through ELISAs using the Receptor

438   Binding Domain (RBD)-specific monoclonal antibody CR3022 [27]. Recombinant Gamma

439   (10795-CV-100) and Delta (10878-CV-100) spike proteins were purchased from R&D Systems

440   (R&D Systems, Bio-Techne, MN, USA).

441

442   **Enzyme-linked immunosorbent assay (ELISA)**

443   Spike-specific IgG in mice sera vaccinated with NDV-HXP-S was measured by ELISA

444   as described previously [23, 28]. Proteins were coated onto Immulon® 4 HBX 96-well

445   microtiter plates (Thermo Fisher Scientific) at 2 µg/mL in 1x coating buffer (SeraCare Life

446   Sciences Inc., MA, USA) at 50 µL/well overnight at 4°C. All plates were washed 3 times with

447   225 µL PBS containing 0.1% (vol/vol) Tween-20 (PBST) and 220 µL blocking solution (3%

448   goat serum, 0.5% non-fat dried milk powder, 96.5% PBST) was added to each well and

449   incubated for 1 hour at RT. Individual serum samples or pooled sera were serially diluted 3-fold

450   in blocking solution followed by a 2-hour incubation at RT at a starting dilution of 1:30. ELISA

451   plates were afterwards washed 3 times with PBST and 50 μL of anti-mouse IgG-horseradish

452   peroxidase (HRP) conjugated antibody (Cytiva, GE Healthcare) was added at a dilution of

453   1:3,000 in blocking solution. After 1 hour, plates were washed 3 times with PBST and

454   developed using SigmaFast OPD (Sigma-Aldrich, MI, USA) for 10 minutes. Reactions were

455   stopped by adding 50 μL 3M hydrochloric acid and absorbance at 492 nm was determined on a

456   Synergy 4 plate reader (BioTek, Agilent Technologies inc., CA, USA) or similar. For each

457   ELISA plate, the blank average absorbance plus 3 standard deviations was used as a cutoff to

458   determine endpoint titers and the area under the curve (AUC) using GraphPad Prism.

459

460   **Microneutralization assays using the authentic SARS-CoV-2 viruses**

461   Microneutralization assays using the authentic SARS-CoV-2 viruses were performed as

462   described previously in Vero-TMPRSS2 [5]. All procedures were performed in a BSL-3 facility

463   at the Icahn School of Medicine at Mount Sinai following standard safety guidelines. Vero-

464   TMPRSS2 cells were seeded in 96-well high binding cell culture plates (Costar, Corning) at a

465   density of 20,000 cells/well in complete Dulbecco's modified Eagle medium (cDMEM) one day

466   prior to the infection. Heat inactivated serum samples (56°C for 1 hour) were serially diluted (3-

467   fold) in minimum essential media (MEM; Gibco) supplemented with 2 mM L-glutamine

468   (Gibco), 0.1% sodium bicarbonate (w/v, HyClone), 10 mM HEPES (Gibco), 100 U/ml

469   penicillin, 100 μg/ml streptomycin (P/S; Gibco) and 0.2% BSA (MP Biomedicals, CA, USA)

470   starting at 1:10. Remdesivir (Medkoo Bioscience inc., NC, USA) was included to monitor assay

471   variation. Serially diluted sera were incubated with 10,000 TCID50 per mL of Wuhan-like WT

472   USA-WA1/2020 SARS-CoV-2, PV29995/2021 (B.1617.2, Delta), MSHSPSP-PV27007/2021

473   (B.1.351, Beta) and PV44488/2021 (B.1.1.529, Omicron) for one hour at RT, followed by the

474   transfer of 120 μl of the virus-sera mix to Vero-TMPRSS2 plates. Infection proceeded for one

475   hour at 37°C and inoculum was removed. 100 μl/well of the corresponding antibody dilutions

476   plus 100 μl/well of infection media supplemented with 2% FBS (Gibco) were added to the cells.

477   Plates were incubated for 48h at 37°C followed by fixation overnight at 4°C in 200 μl/well of a

478   10% formaldehyde solution. For staining of the nucleoprotein, formaldehyde solution was

479   removed, and cells were washed with PBS (pH 7.4) (Gibco) and permeabilized by adding 150

480   μl/well of PBS, 0.1% Triton X-100 (Fisher Bioreagents, MA, USA) for 15 min at RT.

481   Permeabilization solution was removed, plates were washed with 200 μl/well of PBS (Gibco)

482   twice and blocked with PBS, 3% BSA for 1 hour at RT. During this time the primary antibody

483   was biotinylated according to manufacturer protocol (Thermo Scientific EZ-Link NHS-PEG4-

484   Biotin). Blocking solution was removed and 100 μl/well of biotinylated mAb 1C7C7, a mouse

485   anti-SARS nucleoprotein monoclonal antibody generated at the Center for Therapeutic

486   Antibody Development at The Icahn School of Medicine at Mount Sinai ISMMS (Millipore

487   Sigma) at a concentration of 1μg/ml in PBS, 1% BSA was added for 1 hour at RT. Cells were

488 washed with 200 μl/well of PBS twice and 100 μl/well of HRP-conjugated streptavidin (Thermo

489 Fisher Scientific) diluted in PBS, 1% BSA were added at a 1:2,000 dilution for 1 hour at RT.

490 Cells were washed twice with PBS, and 100 μl/well of Sigmafast OPD (Sigma-Aldrich) were

491 added for 10 min at RT, followed by addition of 50 μl/well of a 3 M HCl solution (Thermo

492 Fisher Scientific). Optical density (OD) was measured (490 nm) using a microplate reader

493 (Synergy H1; Biotek). Analysis was performed using GraphPad Prism 7 software. After

494 subtraction of background and calculation of the percentage of neutralization with respect to the

495 "virus only" control, a nonlinear regression curve fit analysis was performed to calculate the

496 50% inhibitory dilution (ID50), with top and bottom constraints set to 100% and 0%

497 respectively. All samples were analyzed in a blinded manner.

498
499 **SARS-CoV-2 plaque assay**

500 Plaque assays with SARS-Cov-2 viruses were performed in the BSL3 facility. Vero-E6

501 cells or Vero-TMPRSS2 were seeded onto 12-well plates in growth media at 1:5 and cultured

502 for two days. Tissue homogenates were 10-fold serially diluted in infection medium (DMEM

503 containing 2% FBS, 100 unit/mL of penicillin, 100 μg/mL of streptomycin (P/S; Gibco) and 10

504 mM HEPES). Two hundred microliters of each dilution were inoculated onto each well starting

505 with a 1:10 dilution of the sample. The plates were incubated at 37°C for 1 h with occasional

506 rocking every 10 min. The inoculum in each well was then removed and 1 mL of agar overlay

507 containing 0.7% of agar in 2 x MEM was placed onto each well. Once the agar was solidified,

508 the plates were incubated at 37 °C with 5% CO_2. Two days later, the plates were fixed with 5%

509 formaldehyde in PBS overnight before being taken out from BSL3 for subsequent staining

510 under BSL2 conditions. The plaques were immuno-stained with an anti-SARS-CoV-2 NP

511 primary mouse monoclonal antibody 1C7C7 kindly provided by Dr. Thomas Moran at ISMMS.

512 An HRP-conjugated goat anti-mouse secondary antibody was used at 1:2000 and the plaques

513 were visualized using TrueBlue[TM] Peroxidase Substrate (SeraCare Life Sciences Inc.)

514
515 **Phylogenetic tree**

516 The phylogenetic tree was built from 3057 SARS-CoV-2 genomes samples between

517 December 2019 and February 2022. Phylogenetic tree and frequency timelines were obtained

518 from the Nextstrain/ncov Project within the GISAID initiative (www.nextstrain.org/ncov) under

519 CC-BY[29, 30].

520
521 **Statistics**

522 A one-way ANOVA with Dunnet multiple comparisons test was used to compare the

523 plaque assay and ELISA biding titers. Statistical analyses were performed using Prism software

524 (GraphPad).

525
526   **Figure legends**
527
528   **Figure 1**:**Evolution of SARS-CoV-2 and appearance of variants of concern (VOC) (A)**
529   Phylogenetic tree (15-Dec-2019 to 06-Feb-2022) with 3057 genomes showing the global
530   evolutionary relationships of SARS-CoV-2 viruses from the ongoing COVID-19 pandemic **(B)**
531   Timeline (15-Dec-2019 to 06-Feb-2022) graph showing the global frequencies by clade of the
532   different SARS-CoV-2 viruses. Graphics were adapted from the website
533   /nextstrain.org/ncov/gisaid/global (accessed 05-Feb-2022 CC-BY [29, 30])
534
535   **Figure 2: Design, production, and characterization of NDV-HXP-S variant vaccines (A)**
536   Structure and design of the NDV-HXP-S construct. The different SARS-CoV-2 spike sequences
537   were introduced between the P and M genes of LaSota L289A NDV strain. The ectodomain of
538   the spike was connected to the transmembrane domain and cytoplasmic tail (TM/CT) of the F
539   protein of the NDV. The original polybasic cleavage site was removed by mutating RRAR to A.
540   The HexaPro (F817P, A892P, A899P, A942P, K986P and V987P) stabilizing mutations were
541   introduced. The sequence was codon-optimized for mammalian host expression. Original
542   WuhanHXP-S sequence is aligned with the new variant constructs: Beta, Gamma and Delta.
543   Changes in the N-terminal domain (NTD), the Receptor Binding Domain (RBD) and in the
544   Spike 2 (S2) with respect to the original WuhanHXP-S sequence are highlighted in red, pink
545   and light purple, respectively. **(B)** NDV-HXP-S variants were rescued by reverse genetics as
546   previously described [24]. Cells were co-transfected with the expression plasmid required for
547   replication and transcription of the NDV viral genome (NP, P, and L), together with the full
548   length NDV cDNA. After 2 or 3 days, the tissue culture supernatants were inoculated into eight-
549   or nine-day-old specific pathogen free (SPF) embryonated chicken eggs. Antigen identity was
550   confirmed by biochemical methods and sequencing. The genetic stability of the recombinant
551   viruses was evaluated across multiples passages on ten days old-SPF embryonated chicken eggs.
552   NDV-HXP-S vaccine was inactivated with BPL and purified by sucrose cushion
553   ultracentrifugation **(C)** Comparison of NDV-HXP-S Delta virus versus NDV-HXP-S Delta with
554   P681R mutation. The spike protein and NDV HN proteins were detected by western blot using
555   an anti-spike 2B3E5 mouse monoclonal antibody and an anti-HN 8H2 mouse monoclonal
556   antibody, respectively. **(D)** Protein staining of NDV-HXP-S variant vaccines resolved on 4-20%
557   SDS-PAGE. The viral proteins were visualized by Coomassie Blue staining (L, S0, HN, N, P
558   and M). The uncleaved S0 spike protein is highlighted in blue with an approximate size of 200
559   kDa.
560
561   **Figure 3: NDV-HXP-S Beta and Gamma induce protective antibodies against homologous**
562   **infection. (A& B)** Design of the study and groups. Eight- to ten-week-old female BALB/c mice
563   were used either vaccinated with 1 µg of total dose of inactivated NDV-HXP-S variant vaccines
564   or WT NDV (negative control). Two immunizations were performed via the intramuscular route
565   (IM) at D0 and D21. At D44, mice were treated with Ad5-hACE2. At D49, mice were
566   challenged with a Wuhan-like (USA-WA1/2020), Beta (B.1.351) or Gamma (P.1) strains and at
567   day two after challenge, lungs were harvested and homogenized in 1 mL PBS and titers were
568   measured by plaque assay on Vero E6 cells. Viral titers in lung homogenates after Wuhan, Beta
569   or Gamma challenge (n=5) **(C).** Viral titers were measured by plaque assay on Vero E6 cells
570   and plotted as Geometric mean titer (GMT) of PFU/mL (limit of detection equals to 50 PFU/mL;
571   a titer of 25 PFU/mL was assigned to negative samples). The error bars represent geometric
572   standard deviation. Geometric mean fold titers over the control are indicated in gray. Spike-
573   specific serum IgG levels against Wuhan spike (n=10) **(D)**, Beta spike (n=10) **(E)**, Gamma
574   spike (n=10) **(F)** and Delta spike proteins (n=5) **(G)**. Antibodies in post-boost (D43) sera
575   samples from the different immunization regimens were measured by ELISA. The GMT of the
576   area under the curve (AUC) were graphed. The error bars represent geometric standard
577   deviation. Statistical difference was analyzed by ordinary one-way ANOVA corrected for
578   Dunnett's multiple comparisons test in all figures (*p < 0.05; **p < 0.01; ***p < 0.001; ****p
579   < 0.0001).

580
581 **Figure 4: Trivalent and tetravalent NDV-HXP-S vaccination regimens induce protection**
582 **against phylogenetically distant SARS-CoV-2 variants. (A&B)** Design of the study and
583 groups. Eight- to ten-week-old female BALB/c mice were used either vaccinated with 1 µg of
584 total dose of inactivated NDV-HXP-S variant vaccines or WT NDV (negative control). Two
585 immunizations were performed via the intramuscular route (IM) at D0 and D21. At D44, mice
586 were treated with Ad5-hACE2. At D49, mice were challenged with Wuhan-like (USA-
587 WA1/2020), Delta (B.1.617.2) or Mu (B.1.621) strains and at day two after challenge, lungs
588 were harvested and homogenized in 1 mL PBS and titers were measured by plaque assay. **(C)**
589 Viral titers after challenge (n=5). Viral titers were measured by plaque assay on Vero E6 cells
590 for Wuhan-like USA-WA1/2020 challenge and Vero-TMPRSS2 cells for Delta and Mu
591 challenges and plotted as GMT of PFU/mL (limit of detection equals to 50 PFU/mL; a titer of
592 25 PFU/mL was assigned to negative samples). The error bars represent geometric standard
593 deviation. Statistical differences were analyzed by ordinary one-way ANOVA corrected for
594 Dunnett's multiple comparisons test. The *p values* and geometric mean fold titers over the
595 control are indicated in blue and gray, respectively. (*p < 0.05; **p < 0.01; ***p < 0.001; ****p
596 < 0.0001) **(D)** Panel of neutralizing activity. Post-boost pooled sera were tested in
597 microneutralization (MNT) assays against Wuhan-like (USA-WA/2020) strain , Delta
598 (B.1.617.2) variant, Beta (B.1.351) variant and Omicron (B.1.1.529) variant in technical
599 duplicates. GMT serum dilutions inhibiting 50% of the infection (ID50) were plotted (limit of
600 detection equals to 10 and was assigned to negative samples). Geometric mean fold change is
601 added in blue.
602
603 **Figure 5: Trivalent and tetravalent NDV-HXP-S vaccination regimens induce broad**
604 **serum antibody titers against phylogenetically distant SARS-CoV-2 variants.** Panel **(A)** and
605 heatmap **(B)** of spike-specific serum IgG against spike variants (n=10). Wuhan, Delta, Alpha,
606 Beta, Gamma and Omicron spikes were used to measure the antibody binding of the different
607 immunization groups. Antibodies in post-boost (D43) sera were measured by ELISAs. GMT
608 AUC is depicted. The error bars represent geometric SD. Geometric mean fold change is added
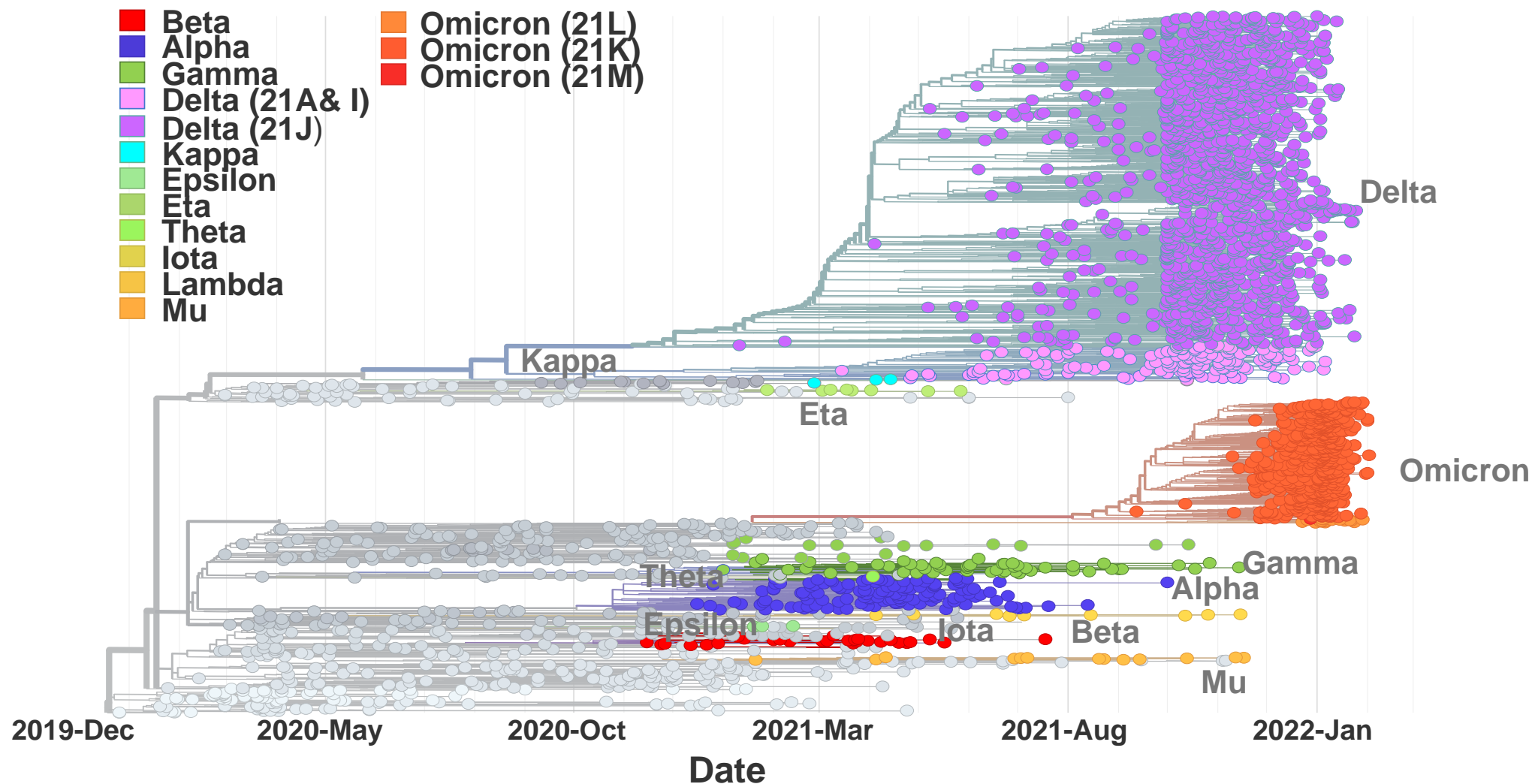609 in blue**.**
610
611
612 **References**
613
614 1.   Carreno, J.M., et al., *Evidence for retained spike-binding and neutralizing*
615   *activity against emerging SARS-CoV-2 variants in serum of COVID-19 mRNA*
616   *vaccine recipients.* EBioMedicine, 2021. **73**: p. 103626.
617 2.   Garcia-Beltran, W.F., et al., *Multiple SARS-CoV-2 variants escape*
618   *neutralization by vaccine-induced humoral immunity.* Cell, 2021. **184**(9): p.
619   2372-2383 e9.
620 3.   Planas, D., et al., *Reduced sensitivity of SARS-CoV-2 variant Delta to antibody*
621   *neutralization.* Nature, 2021. **596**(7871): p. 276-280.
622 4.   Holder, J. *Tracking Coranavirus Vaccination Around the World.* . 2022 [cited
623   2022 05-Febraury-2022]; Available from:
624   https://www.nytimes.com/interactive/2021/world/covid-vaccinations-
625   tracker.html.
626 5.   Carreño, J.M., et al., *Activity of convalescent and vaccine serum against SARS-*
627   *CoV-2 Omicron.* Nature, 2021.
628 6.   Hannah Ritchie, E.M., Lucas Rodés-Guirao, Cameron Appel, Charlie Giattino,
629   Esteban Ortiz-Ospina, Joe Hasell, Bobbie Macdonald, Diana Beltekian and Max
630   Roser. *Coronavirus Pandemic (COVID-19).* 2020 [cited 2022 05-Febraury-
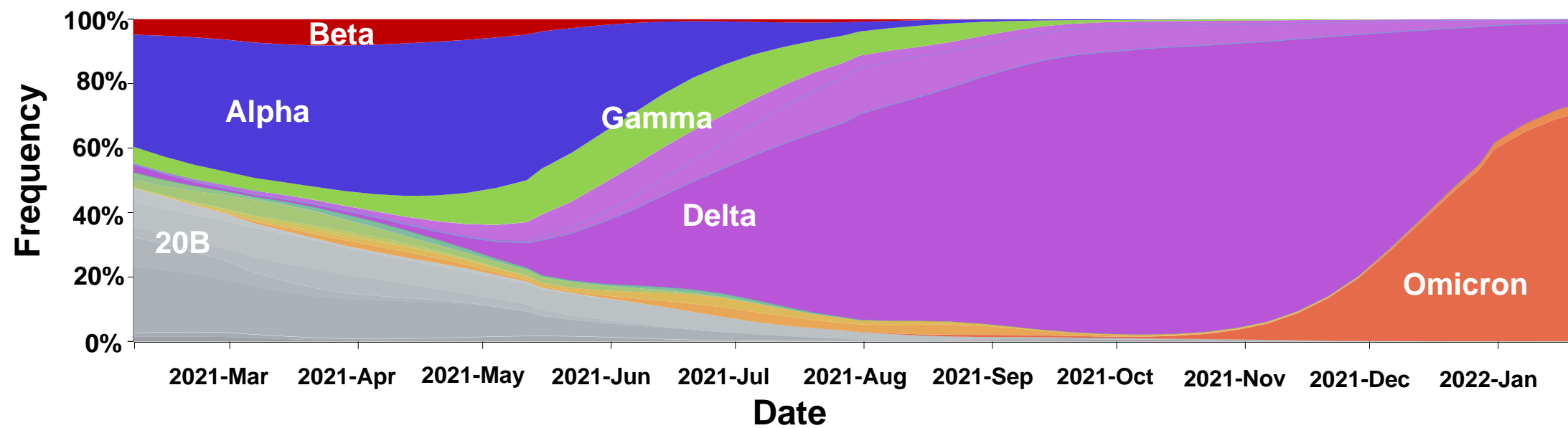631   2022]; Available from: https://ourworldindata.org/covid-vaccinations.

632 7.   Mahase, E., *Omicron sub-lineage BA.2 may have "substantial growth*
633   *advantage," UKHSA reports.* BMJ, 2022. **376**: p. o263.
634 8.   Li, A., et al., *Omicron and S-gene target failure cases in the highest COVID-19*
635   *case rate region in Canada-December 2021.* J Med Virol, 2021.
636 9.   ECDC/WHO, *Methods for the detection and characterisation of SARS-CoV-2*
637   *variants – first update. 20 December 2021*, E.C.f.D.P.a.C.W.H.O.R.O.f. Europe,
638   Editor. 2021: Stockholm/Copenhagen.
639 10.   Sparrow, E., et al., *Global production capacity of seasonal and pandemic*
640   *influenza vaccines in 2019.* Vaccine, 2021. **39**(3): p. 512-520.
641 11.   Sun, W., et al., *A Newcastle disease virus expressing a stabilized spike protein*
642   *of SARS-CoV-2 induces protective immune responses.* Nat Commun, 2021.
643   **12**(1): p. 6197.
644 12.   Hsieh, C.L., et al., *Structure-based design of prefusion-stabilized SARS-CoV-2*
645   *spikes.* Science, 2020. **369**(6510): p. 1501-1505.
646 13.   Tcheou, J., et al., *Safety and Immunogenicity Analysis of a Newcastle Disease*
647   *Virus (NDV-HXP-S) Expressing the Spike Protein of SARS-CoV-2 in Sprague*
648   *Dawley Rats.* Front Immunol, 2021. **12**: p. 791764.
649 14.   Lara-Puente, J.H., et al., *Safety and Immunogenicity of a Newcastle Disease*
650   *Virus Vector-Based SARS-CoV-2 Vaccine Candidate, AVX/COVID-12-*
651   *HEXAPRO (Patria), in Pigs.* mBio, 2021. **12**(5): p. e0190821.
652 15.   Pitisuttithum, P., et al., *Safety and immunogenicity of an inactivated*
653   *recombinant Newcastle disease virus vaccine expressing SARS-CoV-2 spike:*
654   *Interim results of a randomised, placebo-controlled, phase 1 trial.*
655   EClinicalMedicine, 2022. **45**: p. 101323.
656 16.   Samuel Ponce-de-León, M.T., Luis Enrique Soto-Ramírez, Juan José Calva,
657   Patricio Santillán-Doherty, Dora Eugenia Carranza-Salazar, Juan Manuel
658   Carreño, Claudia Carranza, Esmeralda Juárez, Laura E. Carreto-Binaghi, Luis
659   Ramírez-Martínez, Georgina Paz-De la Rosa, Rosalía Vigueras-Moreno,
660   Alejandro Ortiz-Stern, Yolanda López-Vidal, Alejandro E. Macías, Jesús
661   Torres-Flores, Oscar Rojas-Martínez, Alejandro Suárez-Martínez, Gustavo
662   Peralta-Sánchez, Hisaaki Kawabata, Irene González-Domínguez, José Luis
663   Martínez-Guevara, Weina Sun, David Sarfati-Mizrahi, Ernesto Soto-Priante,
664   Héctor Elías Chagoya-Cortés, Constantino López-Macías, Felipa Castro-Peralta,
665   Peter Palese, Adolfo García-Sastre, Florian Krammer, Bernardo Lozano-
666   Dubernard, *Safety and immunogenicity of a live recombinant Newcastle disease*
667   *virus-based COVID-19 vaccine (Patria) administered via the intramuscular or*
668   *intranasal route: Interim results of a non-randomized open label phase I trial in*
669   *Mexico.* medRxiv, 2022.
670 17.   Dang, A.D., et al., *Safety and Immunogenicity of An Egg-Based Inactivated*
671   *Newcastle Disease Virus Vaccine Expressing SARS-CoV-2 Spike: Interim*
672   *Results of a Randomized, Placebo-Controlled, Phase 1/2 Trial in Vietnam.* 2022.
673 18.   Rathnasinghe, R., et al., *Comparison of transgenic and adenovirus hACE2*
674   *mouse models for SARS-CoV-2 infection.* Emerg Microbes Infect, 2020. **9**(1): p.
675   2433-2445.
676 19.   Krammer, F., *SARS-CoV-2 vaccines in development.* Nature, 2020. **586**(7830): p.
677   516-527.
678 20.   Wang, X., et al., *Homologous or heterologous booster of inactivated vaccine*
679   *reduces SARS-CoV-2 Omicron variant escape from neutralizing antibodies.*
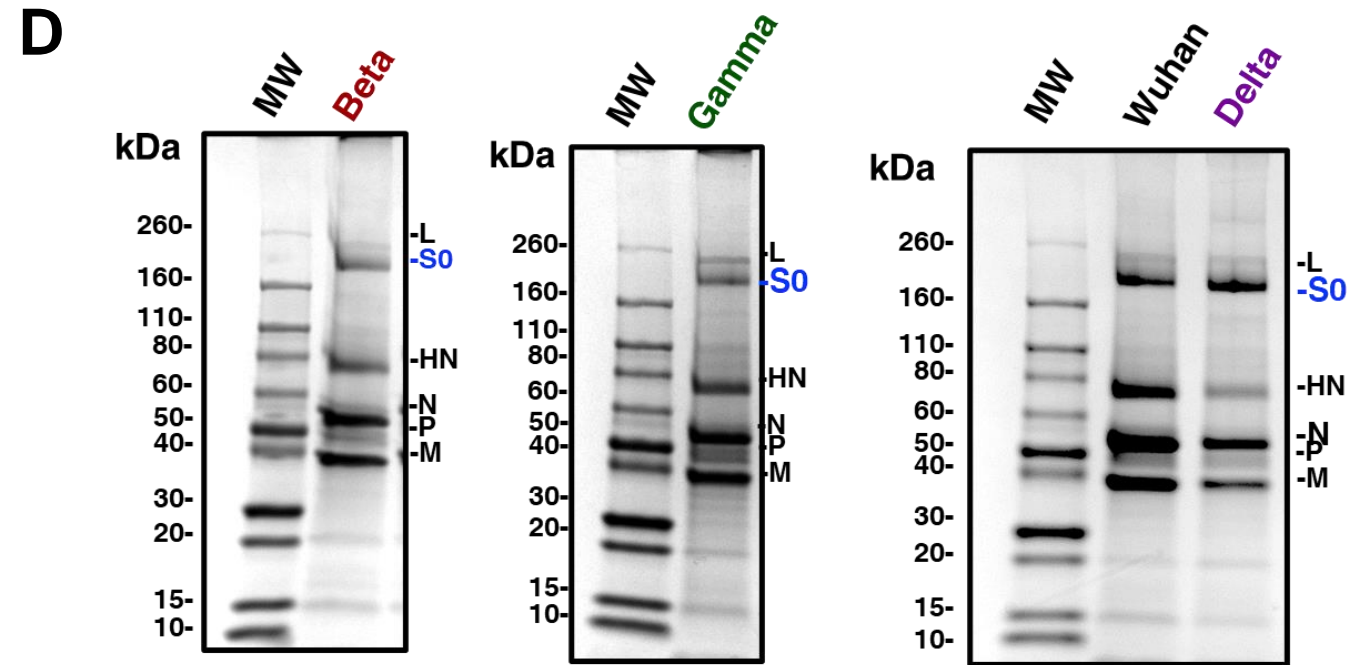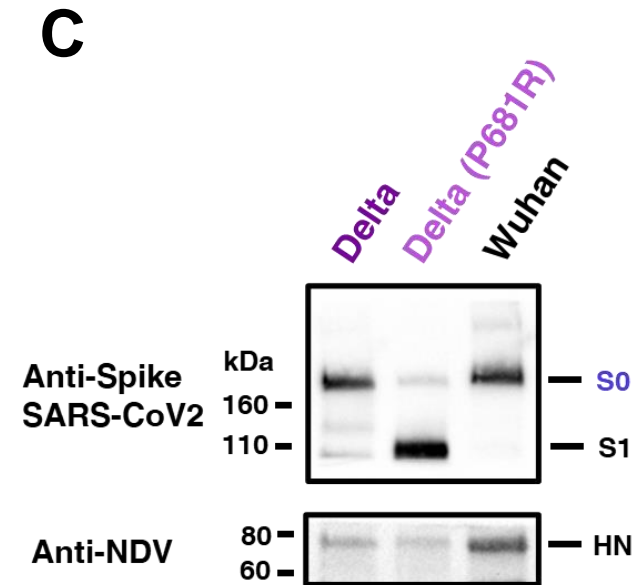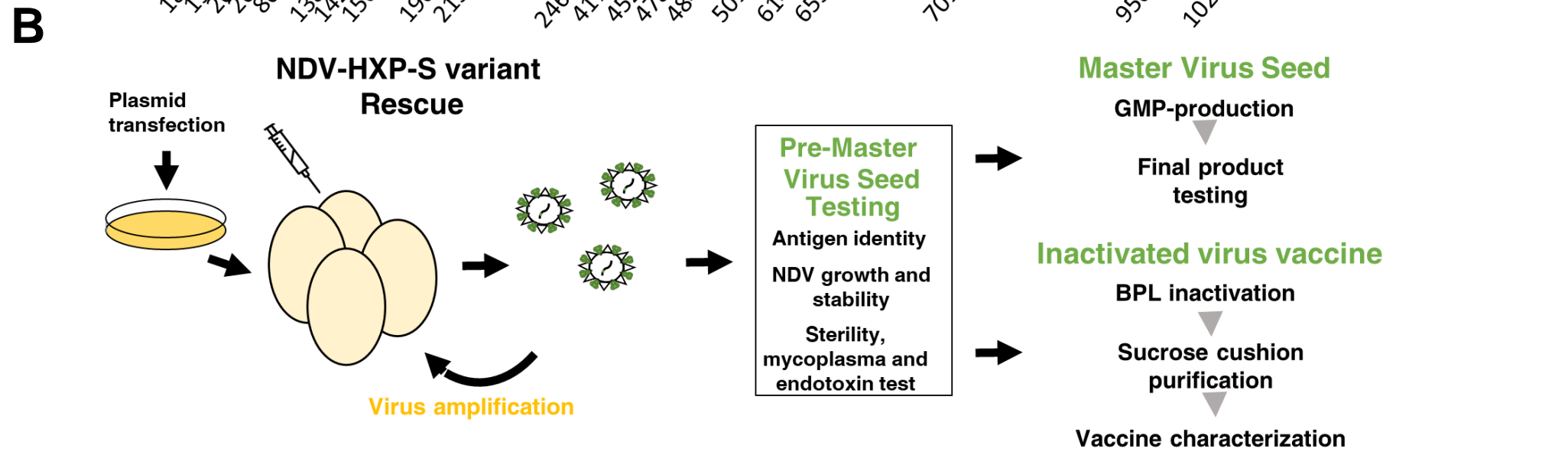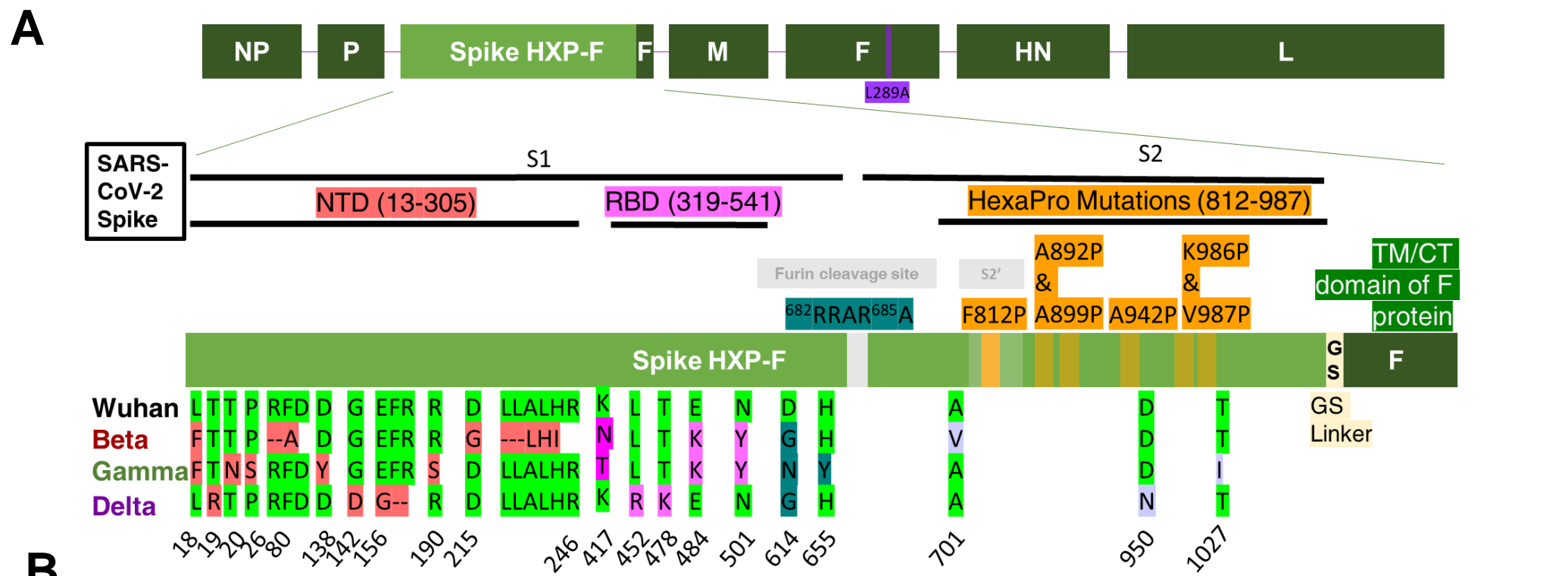680   Emerg Microbes Infect, 2022. **11**(1): p. 477-481.

681 21. Gagne, M., et al., *mRNA-1273 or mRNA-Omicron boost in vaccinated macaques*
682   *elicits comparable B cell expansion, neutralizing antibodies and protection*
683   *against Omicron.* bioRxiv, 2022.
684 22. Ikegame, S., et al., *Fitness selection of hyperfusogenic measles virus F proteins*
685   *associated with neuropathogenic phenotypes.* Proc Natl Acad Sci U S A, 2021.
686   **118**(18).
687 23. Sun, W., et al., *A Newcastle Disease Virus (NDV) Expressing a Membrane-*
688   *Anchored Spike as a Cost-Effective Inactivated SARS-CoV-2 Vaccine.* Vaccines
689   (Basel), 2020. **8**(4).
690 24. Ayllon, J., A. Garcia-Sastre, and L. Martinez-Sobrido, *Rescue of recombinant*
691   *Newcastle disease virus from cDNA.* J Vis Exp, 2013(80).
692 25. Amanat, F., et al., *A serological assay to detect SARS-CoV-2 seroconversion in*
693   *humans.* Nat Med, 2020. **26**(7): p. 1033-1036.
694 26. Stadlbauer, D., et al., *SARS-CoV-2 Seroconversion in Humans: A Detailed*
695   *Protocol for a Serological Assay, Antigen Production, and Test Setup.* Curr
696   Protoc Microbiol, 2020. **57**(1): p. e100.
697 27. ter Meulen, J., et al., *Human monoclonal antibody combination against SARS*
698   *coronavirus: synergy and coverage of escape mutants.* PLoS Med, 2006. **3**(7): p.
699   e237.
700 28. Sun, W., et al., *Newcastle disease virus (NDV) expressing the spike protein of*
701   *SARS-CoV-2 as a live virus vaccine candidate.* EBioMedicine, 2020. **62**: p.
702   103132.
703 29. Hadfield, J., et al., *Nextstrain: real-time tracking of pathogen evolution.*
704   Bioinformatics, 2018. **34**(23): p. 4121-4123.
705 30. Sagulenko, P., V. Puller, and R.A. Neher, *TreeTime: Maximum-likelihood*
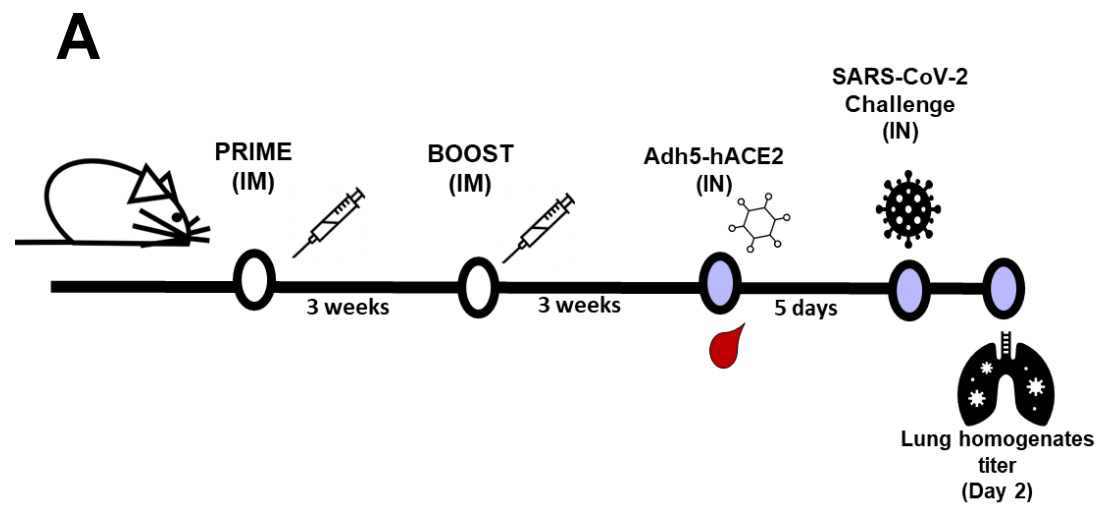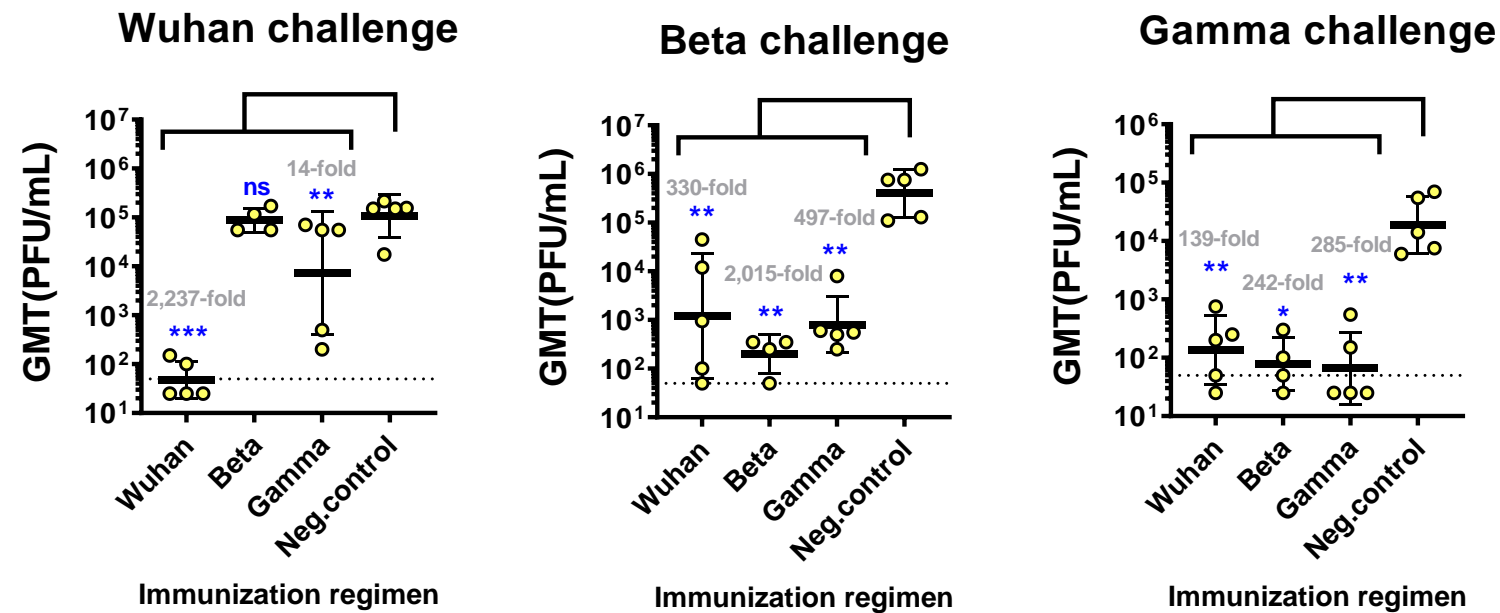706   *phylodynamic analysis.* Virus Evol, 2018. **4**(1): p. vex042.
707

Figure 1

A

B

Figure 2

Figure 3

A

PRIME (IM) — 3 weeks — BOOST (IM) — 3 weeks — Adh5-hACE2 (IN) — 5 days — SARS-CoV-2 Challenge (IN) — Lung homogenates titer (Day 2)

B

Groups	Prime Dose (µg)	Boost Dose (µg)
NDV-HXP-S (Wuhan)	1	1
NDV-HXP-S (Beta)	1	1
NDV-HXP-S (Gamma)	1	1
NDV WT (negative control)	1	1

C **Monovalent vaccination**

Wuhan challenge — GMT(PFU/mL) vs Immunization regimen; ns, **, 14-fold, 2,237-fold, ***

Beta challenge — GMT(PFU/mL) vs Immunization regimen; 330-fold, **, 2,015-fold, **, 497-fold, **

Gamma challenge — GMT(PFU/mL) vs Immunization regimen; 139-fold, **, 242-fold, *, 285-fold, **

D Wuhan Spike (serum IgG) — Geometric mean (AUC); ****, ****
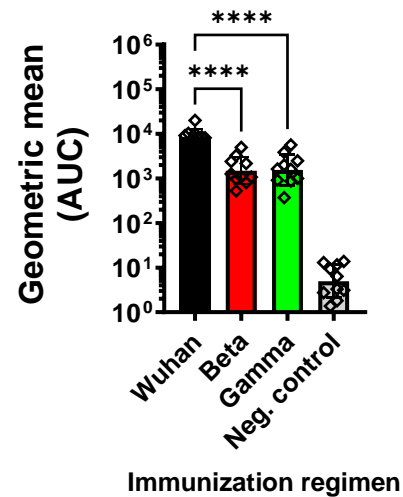
E Beta Spike (serum IgG) — Geometric mean (AUC); ns, ns
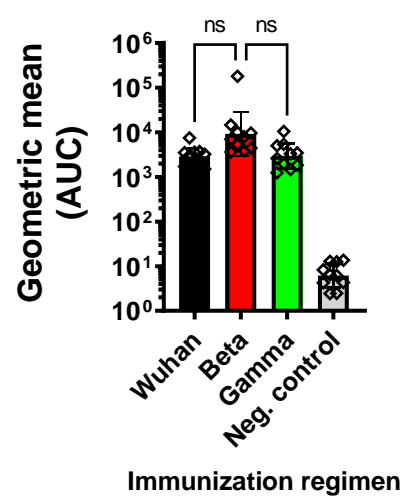
F Gamma Spike (serum IgG) — Geometric mean (AUC); ns, ns

G Delta Spike (serum IgG) — Geometric mean (AUC); *, *

Figure 4

A

PRIME (IM) — 3 weeks — BOOST (IM) — 3 weeks — Adh5-hACE2 (IN) — 5 days — SARS-CoV-2 Challenge (IN) — Lung homogenates titer (Day 2)

B
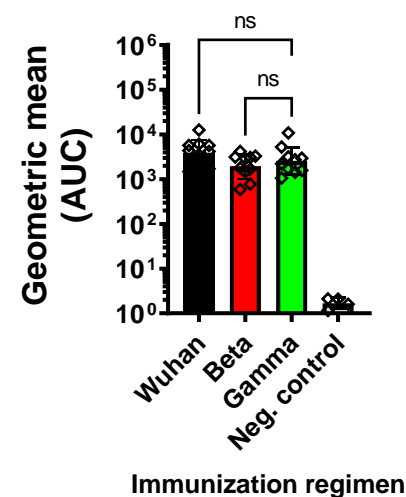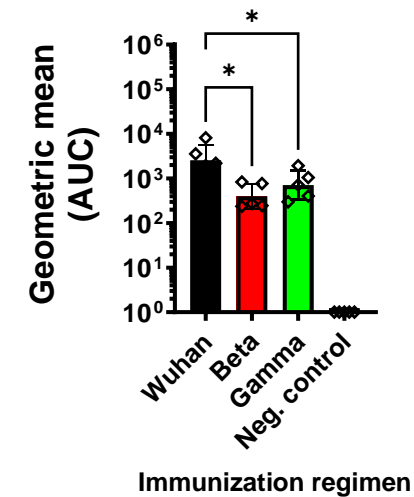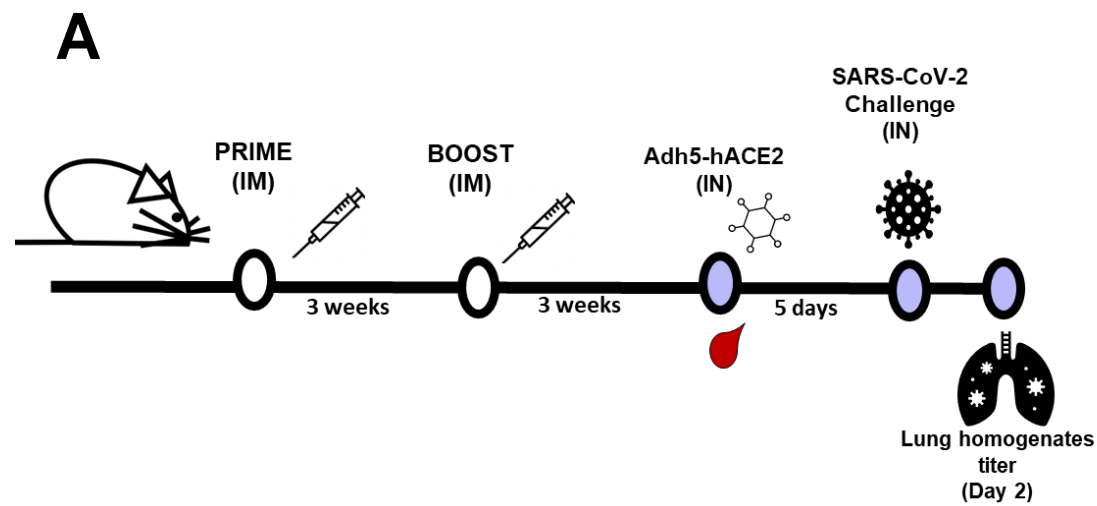
Groups	Prime Dose (µg)	Boost Dose (µg)
NDV-HXP-S (Wuhan)	1	1
NDV-HXP-S (Delta)	1	1
Bivalent NDV-HXP-S (Wuhan+Delta)	0.5 + 0.5	0.5 + 0.5
Sequential (Wuhan /Delta)	1	1
Trivalent NDV-HXP-S (Wuhan+Beta+Delta)	0.33 + 0.33 + 0.33	0.33 + 0.33 + 0.33
Tetravalent NDV-HXP-S (Wuhan+Beta+Gamma+Delta)	0.25 + 0.25 +0.25 + 0.25	0.25 + 0.25 +0.25 + 0.25
NDV WT (negative control)	1	1

C

Multivalent vaccination

Figure 5